

Surface backgrounds in the DEAP-3600 dark matter experiment

B. Cai*, M. Boulay*, B. Cleveland[†], and T. Pollmann* for the DEAP collaboration

**Department of Physics, Queen's University, Kingston, ON K7L 3N6, Canada*

[†]Department of Physics and Astronomy, Laurentian University, Sudbury, Ontario, P3E 2C6, and SNOLAB, Lively, Ontario, P3Y 1M3, Canada

Abstract. DEAP-3600 is a dark matter experiment using 3.6 tons of liquid argon to search for Weakly Interacting Massive Particles (WIMPs), with a target sensitivity to the spin-independent WIMP-nucleon cross-section of 10^{-46} cm². The detector is designed to allow for a three year background-free run with a 1-ton fiducial volume. We identify in this paper the potential sources of surface contamination. We require ²³⁸U and ²³²Th contaminations on the order of 10^{-12} g/g or less, a level achieved by the SNO experiment, and ²¹⁰Pb not significantly out of equilibrium with ²³⁸U, i.e., 10^{-20} g/g or less ²¹⁰Pb in the acrylic vessel or TPB wavelength shifter, which should be achievable with appropriate control of exposure to radon.

Keywords: dark matter, WIMP, liquid argon, backgrounds

PACS: 95.35.+d

INTRODUCTION

The origin of the dark matter in our universe is currently one of the most important questions in particle astrophysics. The DEAP-3600 experiment will use liquid argon for a sensitive dark matter search, with a target sensitivity to the spin-independent WIMP-nucleon cross-section of 10^{-46} cm², more than two orders of magnitude more sensitive than current experiments. This high sensitivity will be achieved due to the very large target mass possible for liquid argon, and the very low backgrounds achievable both in the spherical acrylic detector design, and at the unique SNOLAB facility, the deepest site with the lowest rate of cosmic-ray muons and associated neutron backgrounds at which to perform such an experiment.

A 2-inch thick acrylic vessel (AV) with inner radius 85 cm serves as the primary containment for DEAP-3600 for the 3.6 tons of liquid argon. The inside is coated with tetraphenyl butadiene (TPB, C₂₈H₂₂) wavelength shifter, which serves to shift the ultraviolet (UV) light generated by argon scintillation to the visible region, which can then be transmitted to the photomultiplier tubes (PMTs) through the acrylic. DEAP-3600 plans to use 255 8-inch diameter high quantum efficiency (HQE) tubes, which would allow a light yield of ≥ 6 photo-electrons (pe) per keV_{ee} (electron recoil energy equivalent) deposited in liquid argon. The PMTs are separated from the AV through 18-inch long acrylic light guides. Filler blocks will fill the volume between the light guides, completing the neutron shield, and adding thermal insulation. A stainless steel shell outside of the PMTs permits a dry PMT environment, and acts as a safety barrier in case of failure of the acrylic vessel. An acrylic neck serves to allow access to the interior of the vessel for process systems, calibration sources, and the resurfacer device, a mechanical device to remove the inner surface of acrylic and any implanted radon daughters. The entire detector is housed in an 8 meter diameter water shield to attenuate environmental neutrons generated from the rock wall.

BACKGROUND REQUIREMENT

The target sensitivity for DEAP-3600 will be achieved with an essentially background-free exposure of 1,000,000 kg-days in our energy region of interest (ROI). The energy threshold in liquid argon above which we have good separation between WIMPs and backgrounds is around 20 keV_{ee} [1]. For background estimates in this paper, we use a nominal analysis window of 20–40 keV_{ee}, which corresponds to nuclear recoil energies between 80 and 160 keV_r with a measured value of 0.25 as the nuclear recoil quenching factor in liquid argon [2]. There are three primary classes of backgrounds which can mimic a dark matter particle interaction: β/γ events, neutrons, and alpha decays. The dominant source of β decays in this experiment will be from radioactive ³⁹Ar that is present in natural argon condensed from

TABLE 1. DEAP-3600 background budget in 3 years, where in addition to fiducial volume cut, β 's can be further distinguished from WIMP events by pulse-shape discrimination

Background	Raw No. Events in Energy ROI	Fiducial No. Events in Energy ROI
Neutrons	30	< 0.2
Surface events	150	< 0.2
^{39}Ar β 's	1.6×10^9	< 0.2

the atmosphere. Very good discrimination of β events from nuclear recoils is possible in argon by using pulse-shape discrimination (PSD) because of very different scintillation time spectra for these two event types [3]. The inner argon target is well-shielded from neutron backgrounds, surrounded by 50 cm of acrylic and other plastic, which acts as a passive shield for neutrons generated in the photomultiplier array.

This paper focuses on backgrounds from alpha decays, the third class of backgrounds in DEAP-3600, which are generated either from radioactive impurities in the detector materials or from radon emanation. Alpha particles do not travel very far in materials before losing all their energy. An α decay in the central liquid argon region can easily be tagged because of its high energy deposition, and it is not a source of backgrounds in our low energy analysis window. We are concerned with backgrounds from surfaces since there we may only observe either a fraction of the α -particle's energy, the recoiling nucleus, which is close to our energy region of interest, or both.

Table 1 shows the background budget for DEAP-3600 used to set tolerable backgrounds and impurity levels. It requires background events in the energy region of interest for the WIMP search from each source of events are < 0.2 events in 3 years¹, reconstructed in the fiducial 1000-kg volume. Surface backgrounds will be reduced in the final DEAP-3600 analysis by applying position reconstruction to define an inner fiducial volume. To set our tolerable surface background rates, we have used a conservative estimate of $\sigma = 10$ cm for the position reconstruction resolution of events near the analysis energy threshold of 20 keV_{ee}. With this estimate, an efficiency of approximately $\epsilon = 1.35 \times 10^{-3}$ is found for surface events (at $R = 85$ cm) to reconstruct inside the fiducial region ($R = 55$ cm). A more sophisticated event vertex fitter has shown better background suppression than this baseline value. Monte Carlo simulations were used to generate surface events and the triggered PMT spatial hit and charge patterns were fitted using a maximum-likelihood estimator. We expect to meet or exceed our suppression factor with a 1 ton fiducial volume.

We have nonetheless assumed the nominal fiducial volume to get the target background levels for surface events in this paper. For each of the potential contributing sources and for the purpose of calculation, we allow 0.01 background events in the fiducial volume in 3 years², in order to meet the requirement of a total of 0.2 background budget. Therefore we can tolerate for each individual source a maximum of

$$N = 0.01/\epsilon = 7.4 \quad (1)$$

background events in the full liquid argon volume.

SOURCES OF SURFACE BACKGROUNDS

Figure 1 depicts typical α decays which can occur in different regions of the detector. An α decay in the bulk argon, i.e., case (a), can be tagged by the full-energy deposition of the α , which will be above several MeV and so outside of our energy region of interest. The most problematic decays are those on the detector surface. In case (b) a decay ejects a recoil nucleus into the liquid argon, and the backwards-going α particle generates light in the TPB layer. In DEAP-3600 we would see both signals as a single event and the detected signal will have some probability of contaminating the energy region of interest. In case (c) the α particle instead enters the liquid argon, and the recoil nucleus is ejected into the TPB. In this case we would see the full α energy in the argon. This signal is thus expected to be outside of the energy region of interest, and we can use it as a calibration of the background rate from particular α emitters. In case

¹ 0.2 is chosen so that it would allow a total of less than 1 event leakage in 3 years.

² Likewise, 0.01 is chosen as a number that is sufficiently smaller than 0.2, to account for various sources that may contribute to the overall background budget.

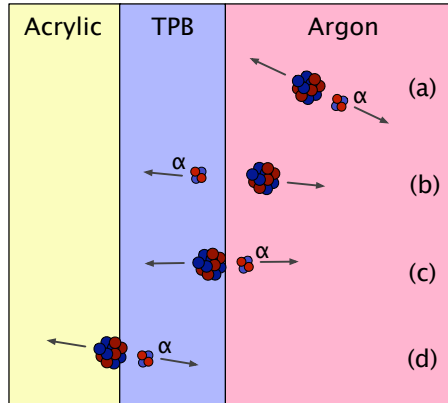


FIGURE 1. Alpha decays in the DEAP detector. Four example cases are shown: (a) An α decay in the bulk argon region can be tagged by the full α energy. (b) An α emitter on the inner TPB surface can eject a recoil nucleus into the argon and an α into the TPB, leading to a low-energy event which includes light from α scintillation in TPB and from the recoil in argon. (c) An α emitter on the inner TPB surface can eject an α into the argon. In this case the full α energy is seen in the argon. (d) shows an event from impurity in the TPB or acrylic, which can lead to a continuum of low-energy events from α particle scintillation in the TPB

(d) a decay from the bulk TPB or acrylic region can lead to a small signal (in the energy region of interest) either from α energy deposited in the TPB, or from residual α energy deposition on the liquid argon region.

Alphas from the acrylic vessel surface layer or the TPB wavelength shifter can therefore lead to leakage events in the WIMP energy region of interest. Sources of α decays include long-lived radioactive impurities in the detector materials, for example ^{238}U , ^{232}Th and their daughters, as well as radon progenies on the inner detector surfaces or inside the AV surface layer. Surfaces exposed to ^{222}Rn can accumulate the long-lived daughter ^{210}Pb , leading to the eventual α decay of ^{210}Po . Radon emanation from the detector process system and other components leads to alpha decays in liquid argon and some of their daughters migrate onto the TPB surface. We must therefore control the total radon emanation rate into the active region. In addition, ^{210}Pb could desorb from the process system and later adsorb to the inner detector surface. We need strict cleanliness control on all components that will be wetted with the liquid argon. The following is a list of all the potential sources of these surface backgrounds:

1. ^{238}U , ^{232}Th , and ^{210}Pb in the bulk acrylic of the AV (we are sensitive to only the inner 80 microns);
2. ^{238}U , ^{232}Th , and ^{210}Pb in the TPB;
3. ^{210}Pb deposited on the AV inner surface (touching TPB) from ^{222}Rn exposure;
4. ^{210}Pb deposited on the TPB inner surface (touching liquid argon) from ^{222}Rn exposure or radon emanation;
5. ^{210}Pb desorbed from the process system or other components that later adsorbs to the inner detector surface;
6. Alpha decays from the detector neck region;
7. Alpha decays from particulates in the liquid argon.

For 1–4 we first calculate in the next chapter the probability of event leakage into the WIMP energy ROI. Using the background requirement defined in (1), we can then set a target limit for each of the listed impurities. ^{210}Pb desorption and neck events are discussed later in the paper. Particulates in the liquid can be removed with recirculation and purification of the liquid argon in DEAP-3600 and they are therefore of less concern.

TARGET LEVEL FOR MATERIAL PURITY

Simulations were performed in order to estimate the probability for surface background events to generate leakage in our WIMP energy region of interest, that is, to deposit equivalent of 20–40 keV_{ee} energy in liquid argon. Alphas from ^{232}Th , ^{238}U , as well as ^{210}Pb decay chains, assuming secular equilibrium, are generated in the surface layer of

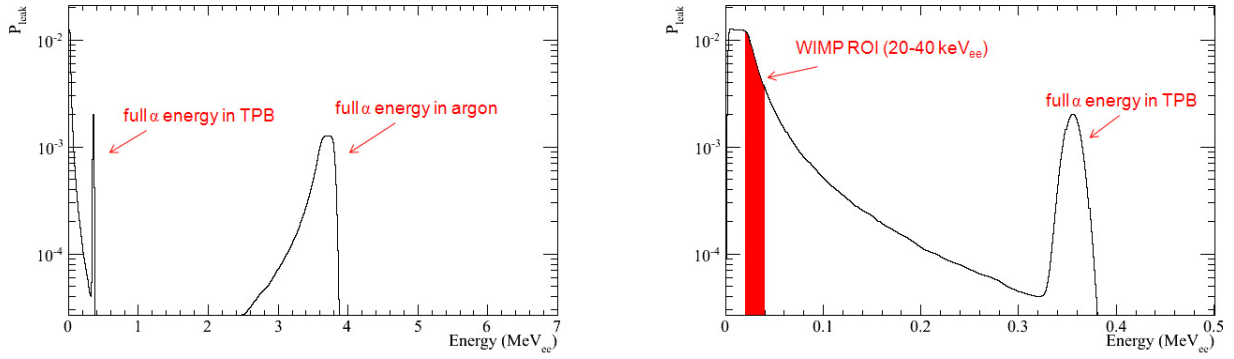


FIGURE 2. Energy deposition in liquid argon from ^{210}Po decays in the TPB. It is assumed that the recoiling 103.1 keV ^{206}Pb nuclei deposit all their energy in the TPB since their range is $< 0.1 \mu\text{m}$. The x-axis is in electron recoil equivalent energy and the y-axis is the fraction of events per 1 keV_{ee} energy bin

different materials. The thickness of TPB used in the simulation is $3 \mu\text{m}^3$. Energy loss of the α particles and their recoiling nuclei along their path was calculated according to SRIM [4]. The α energy deposition in liquid argon (E_1) and in TPB (E_2), as well as recoiling nucleus energy deposition in liquid argon (E_3) and in TPB (E_4), are then recorded for each event. The expected total energy deposition in liquid argon is from the sum of all four contributions:

$$E = E_1 \cdot L_{eff\alpha} + E_3 \cdot L_{effr} + E_2 \cdot Y_2/Y + E_4 \cdot Y_4/Y \quad (2)$$

where E is in unit of MeV_{ee}. $L_{eff\alpha} = 0.72$ is the alpha quenching factor in liquid argon [5] and $L_{effr} = 0.25$ is the nuclear recoil quenching factor in liquid argon. $Y = 6000 \text{ pe/MeV}_{ee}$ is the estimated light yield in liquid argon for DEAP-3600. $Y_2 = 400 \text{ pe/MeV}$ is the estimated α light yield in TPB for DEAP-3600⁴. $Y_4 = Y_2 \cdot L_{effr}/L_{eff\alpha} = 139 \text{ pe/MeV}$ is the light yield in TPB assumed for nuclear recoils.

Figure 2 shows the simulated energy spectrum in liquid argon in the DEAP-3600 detector when ^{210}Po decays inside the TPB⁵. We can note that approximately 43.6% of decays lead to a full-energy α peak in the liquid argon, and approximately 14.7% of the decays lead to a background event in the energy region of interest. It should also be noted that there exists a peak corresponding to the full energy of the α particle in the TPB layer (at approximately 0.36 MeV_{ee}). The probability for an α decay in TPB to generate a background event in the energy region of interest, defined as P_{eak} , will be used to set tolerable limits for ^{210}Po in TPB.

Table 2 summarizes for each source the leakage rate and the target level of impurities R , which is calculated from the following formula:

$$R = \frac{N}{m \cdot t \cdot n \cdot P_{\text{eak}}} \quad (3)$$

where $N = 7.4$ is the maximum number of background events from each source calculated in (1). $m = 0.864 \text{ kg}$ is the mass of inner 80 microns of AV and $m = 0.031 \text{ kg}$ for 3 microns of TPB. m is replaced with $A = 9 \text{ m}^2$, the area of the TPB surface, to calculate the limit in the last row of Table 2. $t = 3 \text{ years}$ is the planned experiment livetime. $n = 8, 5.99, \text{ and } 1$ is the total number of alphas generated in each $^{238}\text{U}, ^{232}\text{Th}, \text{ and } ^{210}\text{Pb}$ decay chain, respectively. The target impurity limits are shown in both $\mu\text{Bq/kg}$ and ppt⁶. Alphas from ^{210}Po decays on the inner surface of the AV (in between AV and TPB) either go into acrylic, with the recoiling nuclei leaving essentially no signal in the TPB,

³ This TPB thickness optimizes the light yield in DEAP-3600.

⁴ It was measured that alpha light yield in TPB is 71 pe/MeV with a setup which uses a 5-inch ETL 9390B PMT and has a 35% geometric acceptance [6]. It is estimated that in DEAP-3600, the light yield can be increased by a factor of 2 using higher Quantum-Efficiency PMTs, and the geometric acceptance will be $\sim 100\%$. Therefore, alpha light yield in TPB for DEAP-3600 is around $2 \times 71/0.35 = 400 \text{ pe/MeV}$.

⁵ The histogram in the figure includes the effect of energy resolution.

⁶ The conversion is $1 \mu\text{Bq/kg} = 0.08, 0.25, \text{ and } 3.54 \times 10^{-10} \text{ ppt}$ for $^{238}\text{U}, ^{232}\text{Th}, \text{ and } ^{210}\text{Pb}$, respectively.

or produce large scintillation signals since the alpha particles will deposit some energy in the TPB and the rest in the liquid argon. Neither case introduces leakage in the WIMP energy ROI.

The uncertainty shown in the table is an example of one of the systematic uncertainties, i.e., $\pm 20\%$ systematic uncertainty in the measurement of alpha scintillation light yield in the TPB. It leads to at most a 20% increase in the probability of leakage except in the case when ^{210}Pb decays on the inner surface of TPB a low energy peak around WIMP energy ROI leads to a large increase of leakage probability. The largest leakage probability is used to calculate the impurity limit for each source. Other systematics that are not in the table include the uncertainty in the TPB thickness, DEAP-3600 solid angle for TPB light emission, etc. These uncertainties would lead to a very small reduction to the fiducial mass of DEAP-3600, therefore having a negligible effect to our overall physics sensitivity.

TABLE 2. Summary table for estimated probability of leakage in the WIMP energy ROI per alpha decay in ^{238}U , ^{232}Th , and ^{210}Pb decay chains assuming secular equilibrium. The uncertainty in the third column comes from varying light yield in the TPB by $+20\%$ (shown in the upper corner) and -20% (lower corner). This effect is very small when the decays are inside AV since only a small fraction of alphas can reach the AV surface and deposit energy in TPB. When the decays are inside TPB, more light in TPB pushes the energy spectrum to the right (harder spectrum) which leads to more leakage events. When the decays are on the inner surface of TPB, it so happens that more TPB light yield pushes the low energy peak away from WIMP energy region. The limits are calculated with the maximum leakage probability for each source, i.e., sum of the two numbers with the + sign for each case

		Prob. of leakage (%)	Limit ($\mu\text{Bq/kg}$)	Limit (ppt)
Inside AV	^{238}U	$0.28^{+0.02}_{-0.01}$	3.9	0.3
	^{232}Th	$0.27^{+0.03}_{-0.02}$	5.2	1.3
	^{210}Pb	$0.27^{+0.02}_{-0.01}$	31.2	1.1×10^{-8}
Inside TPB	^{238}U	$12.4^{+1.5}_{-2.2}$	2.3	0.2
	^{232}Th	$11.6^{+1.7}_{-2.2}$	3.2	0.8
	^{210}Pb	$14.7^{+1.3}_{-3.0}$	15.8	5.6×10^{-9}
On AV surface	^{210}Pb	0	-	-
On TPB surface	^{210}Pb	$0.2^{+0.2}_{-11.2}$	$0.1 \mu\text{Bq/m}^2$	-

ACRYLIC ASSAY

Sample acrylic from RPT has been recently assayed at SNOLAB with a Ge gamma detector. It is a coaxial detector that measures samples placed outside its endcap. The sensitivity of this detector is around 10 ppt for ^{238}U and ^{232}Th and it is not sensitive to ^{210}Pb since its low energy gamma cannot penetrate the detector endcap. The upper limit of the impurities in the RPT samples and the corresponding maximum number of leakage events are shown in Table 3.

We plan to assay bulk acrylic for radioactive contaminants, namely ^{238}U , ^{232}Th , and ^{210}Pb , at the required level using new a two-furnace system and a new Ge well detector. Large samples of acrylic (around 10 kg) can be vaporized with this system and their residues counted for sensitive assays. The count rates, assuming the impurity concentrations in the acrylic are equal to the maximum allowable concentrations in Table 2, are given in the last column of Table 4. Although these rates are very low, it will be possible to detect a signal if the counter background is comparable with the best HPGe detectors in literature [7, 8, 9]. It should be noted that the acrylic assay will be used to verify the acrylic

TABLE 3. Assay results from SNOLAB gamma counting and estimated leakage in 3 years of DEAP-3600 data taking. The number of background events is calculated from comparing the assay results with the required radiopurity level in Table 2

	Assay (ppt)	Estimated leakage events in 3 years in ROI
^{238}U	< 9.6	< 0.32
^{232}Th	< 16.8	< 0.13

background levels after AV production, since we will be building the AV before the middle of 2011. We expect the levels will be below targets⁷.

TABLE 4. Assumed maximum acceptable concentrations and their implied count rates. Decay rates and estimated count rates are based on vaporization of 10 kg of acrylic and assume no losses in chemical processing. Counting efficiency assumes sample is measured in a well detector

Radioactive isotope	Limit (ppt)	Decay rate (decays/day)	E_γ (keV)	Branching ratio	Counting efficiency	Count rate (counts/day)
²³⁸ U	0.3	3.4	351.9	0.358	0.4	0.49
²³² Th	1.3	4.5	238.6	0.433	0.6	1.17
²¹⁰ Pb	1.1×10^{-8}	27.0	46.5	0.0425	0.9	1.03

We plan to oversee the acrylic fabrication process in the factories to make sure that the acrylic vessel is produced in a clean environment. The TPB wavelength shifter will be purified. We will remove surface contamination from the acrylic vessel inner surface using a resurfacer device and the vessel will be sealed from air contact during and after sanding. Only materials that have low radon emanations will be selected for the DEAP-3600 process systems and a radon trap will be in place for removing radon from argon gas, or any other gas that will be used to purge the detector inner volume.

RADON EMANATION

There are two particularly problematic decays in the ²³⁸U chain below ²²²Rn: ²¹⁴Po and ²¹⁰Po. From DEAP-1, ²¹⁴Po from ²²²Rn decays are seen to plate out on the detector surface. Further down the chain ²¹⁰Po is expected to be a source of background due to buildup of the long-lived isotope ²¹⁰Pb. The following calculation can be used to set a limit on the allowable radon emanation load into the DEAP-3600 central detector region. For these calculations, we assume a constant emanation rate of ²²²Rn into the central argon region, R_{Rn} , from all sources. ²¹⁴Po is expected to be in equilibrium with ²²²Rn, so that the background rate in the energy region of interest due to ²¹⁴Po α decays is given by R_{LE} (from ²¹⁴Po) = $R_{Rn} \cdot P_{leak}$, where R_{LE} is the rate of low energy background events and P_{leak} is the probability of a ²¹⁴Po decay on TPB inner surface generating a low energy background event. The allowable ²²²Rn emanation rate

$$R_{Rn} \leq \frac{R_{LE}}{P_{leak}} = 14 \mu\text{Bq} \quad (4)$$

where $R_{LE} = 0.2/\varepsilon/t = 1.6 \mu\text{Bq}$. 0.2 is our background budget in $t = 3$ years and $\varepsilon = 1.35 \times 10^{-3}$ is the fraction of surface events reconstructed in the fiducial volume. We use $P_{leak} \approx 11.4\%$ in the calculation which is the probability of a ²¹⁰Po decay on TPB inner surface generating a low energy background event.

In addition to the prompt ²²²Rn decay of ²¹⁴Po, ²¹⁰Pb will build up over time, since it has a lifetime that is long compared to the experiment duration. The maximum radon emanation rate for a given low energy background rate

$$R_{Rn} = \frac{R_{LE}}{P_{leak}} \cdot \frac{\tau_{210\text{Pb}}}{t} = 151 \mu\text{Bq} \text{ (steady-state radon emanation limit)} \quad (5)$$

using $R_{LE} = 1.6 \mu\text{Bq}$, $P_{leak} = 11.4\%$, $\tau_{210\text{Pb}} = 32.2$ years, and $t = 3$ years. We have neglected the decay of ²¹⁰Pb since $t \ll \tau_{210\text{Pb}}$. The time required for the ²¹⁰Po rate to reach equilibrium with the ²¹⁰Pb rate is also neglected. After approximately two years the ²¹⁰Po decay rate will be 70% of the ²¹⁰Pb decay rate [11].

Several subsystems such as the resurfacer and the glove box are planned to be deployed or open to the central volume for a much shorter time. In this case we are only sensitive to the backgrounds due to buildup of ²¹⁰Pb, since we will not see the first three α 's below ²²²Rn. Table 5 summarizes the tolerable radon emanation loads given by (5) for the resurfacer, the glove box, and the TPB applicator device, assuming specific values for the exposure time to the inner detector region for each. It should be noted that in the case of the glove box and TPB applicator active vacuum pumping and/or purging of the inner region may occur, and so the tolerable radon loads should be corrected to include

⁷ For reference, the vaporization assay results from SNO give < 0.73 ppt of ²³⁸U and < 0.11 ppt of ²³²Th [10].

TABLE 5. Radon emanation target specifications for the resurfacer, glove box, TPB applicator, and purifiers with assumed exposure times. If additional purging or vacuum pumping is supplied (possible for the glove box and TPB applicator), then the above targets should be appropriately corrected (for both source terms and efficiency of radon removal). These limits should be readily achievable with careful materials selection and cleaning. The limits set for the radon trap and SAES purifier are for a one-time only purification run of each independently. For continuous operation (of either in parallel) the overall 14 μBq limit would apply

Component	Target ^{222}Rn emanation rate	Exposure time
Resurfacer	5.4 mBq	1 month
Glove box	21.7 mBq	1 week
TPB applicator	21.7 mBq	1 week
Radon trap & SAES purifier	5.4 mBq	1 month

additional sources of radon (in the case of purging) and the effectiveness of radon removal (for both vacuum pumping and purging). The process system will also include a radon trap and a SAES purifier, and should allow continuous filtration of argon for particulate removal. If the radon trap and SAES purifier are run continuously, the target of 14 μBq will apply to that combined system (although in that case would be dominated by the outlet of the radon trap and process components between the outlet and detector volume). If the radon trap and/or SAES purifier are only operated during the initial cool down and fill, then the emanation requirements are reduced, as seen in Table 5.

DEAP-1 BACKGROUND STUDIES

DEAP-1 is a prototype detector with a 7 kg target of liquid argon. The detector consists of an inner acrylic cylinder coated with TPB wavelength shifter, 20 cm long ultraviolet transmitting (UVT) acrylic light guides on the side, and two PMTs attached to the light guides and operated at room temperature. The target chamber is surrounded by a neutron and γ -ray shield consisting of a minimum of two layers of ultra-pure water in 12-inch cubical polyethylene containers, for a total water shielding thickness of 60 cm. DEAP-1 was operated during 2006 – 2007 at Queen’s university for demonstration of pulse-shape discrimination. The detector was then moved to underground at SNOLAB in November 2007 and has had a number of successful data runs with liquid argon.

DEAP-1 has successfully reduced backgrounds through a series of detector improvement. The first generation clean chamber (v1) was installed for the July 2008 run. This chamber was produced in a glove box at Queen’s with radon-reduced air. The second-generation clean chamber (v2) using improved glove-box techniques, production with cleaner materials, and improved handling on site resulted in rates of approximately 0.2 mHz in the WIMP energy ROI. A series of ^{222}Rn emanation tests showed that this improvement is attributable to using a Gore-tex reflective coating instead of a Bicon reflective paint. A radon trap was installed in the system to filter radon from argon gas during detector filling.

The third-generation chamber (v3) was coated with purified acrylic, and high Quantum-Efficiency 8-inch PMTs were installed for this run. The light yield has been increased to 4.7 pe/keV, almost a factor of 2 compared to using 5-inch PMTs. The background rate in 120 – 240 pe stayed at around 130 μBq which is expected if the source of these events is internal radon emanation. A calibrated radon spike was introduced in September 2010 in order to study the correlation of high energy alphas from radon decays and low energy leakage events.

We can use the DEAP-1 data to determine an upper limit on the amount of ^{210}Pb in acrylic. From the v2 chamber⁸, we saw approximately 40 events in the ^{210}Po alpha region for 240 hours of livetime, so $R < 40/240$ hours. From SRIM simulation of ^{210}Po alphas in an 80 micron layer of AV, we should see approximately 2.3% of those events (above 3 MeV_{ee}). Table 6 summarized the upper limit we can set on the ^{210}Pb rate in acrylic using these numbers⁹.

Note that the DEAP-1 process system has been exposed to SNOLAB mine air during assembly and ^{210}Pb has built up on the surfaces. The rate of ^{210}Pb deposition on surfaces from exposure to radon-laden air has been studied extensively by the medical community. Although the actual deposition rate depends on many factors, including aerosol concentration in the room environment, relative humidity and air velocity, we use an average deposition rate of

⁸ This was McMaster-Carr acrylic (same as for the v3 chamber), not RPT.

⁹ This rate is not inconsistent with backgrounds from ^{222}Rn in the argon. However, all we can do is to set an upper limit on ^{210}Pb .

TABLE 6. Upper limit on ^{210}Pb in the DEAP-1 acrylic chamber

Parameter	Value
Max. rate of ^{210}Po alphas in DEAP-1	2×10^{-3} Bq
Mass of 80 micron surface layer in DEAP-1	0.017 kg
$R_{210\text{Pb}}$ = Max. rate of ^{210}Pb per kg of acrylic	0.118 Bq/kg
Max. concentration of ^{210}Pb in DEAP-1 acrylic	4.2×10^{-5} ppt

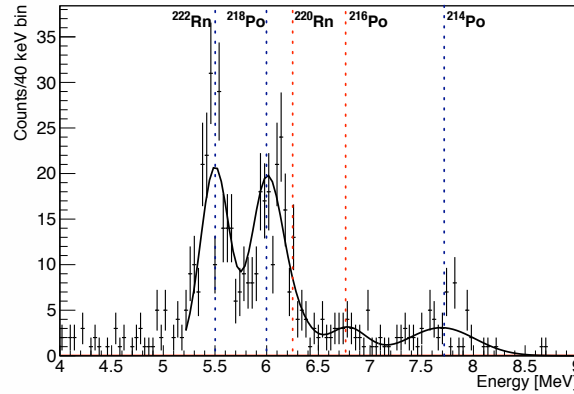


FIGURE 3. High energy spectrum and fit for v3 low voltage data. The peaks line up with radon decay daughters

0.001 Bq/m^2 ^{210}Po per Bq/m^3 of ^{222}Rn per year of exposure [11]. With the ^{222}Rn level at SNOLAB $\sim 100 \text{ Bq/m}^3$ [12], we can estimate the ^{210}Po activity of surfaces exposed to SNOLAB air:

$$\text{Rate of } ^{210}\text{Po} = 3.17 \times 10^{-9} \text{ Bq/m}^2/\text{s} \quad (6)$$

If all of the ^{210}Pb was transferred to the DEAP-1 inner detector region, an exposure to one square meter of surface for approximately 7 days would be sufficient to generate 2×10^{-3} Bq of the ^{210}Po alphas we saw in DEAP-1 data. Although the desorption of ^{210}Pb from surfaces is not likely to be total, there will likely be some desorption into the inner detector region, and so it is reasonable to plan to wash all surfaces that will be wetted with argon (gas or liquid) of ^{210}Pb . The Borexino collaboration has placed significant effort in understanding desorption of ^{210}Pb for purity of their inner nylon vessel [13]. Citric acid has also been used to both passivate metals and to remove radon daughters [14] and may be a suitable cleaning solution for the DEAP-1 process system (as well as the DEAP-3600 process system, and possibly the acrylic vessel and other detector components), although further study is required.

Figure 3 shows the high energy part of the background spectra for the v3 data set. The spectrum was fitted assuming that the high energy spectrum is due to decays of ^{222}Rn , ^{218}Po , ^{214}Po , ^{220}Rn , and ^{218}Po . The energy for each of the decays is fixed, the number of events in each chain, resolution, and ^{214}Po scaling factor are fitted. The number of ^{214}Po had to be reduced by a scaling factor, presumably because it or one of its predecessors adheres to surfaces of the detector, such that at least half of the decays go into the acrylic vessel and are thus not detected at high energies.

Increasing the amount of radon in the detector with a calibrated radon spike leads to an increase of rate at all energy regions. Only $\sim 3\%$ of the rate increase at full energy is seen in the low energy region of interest, which means most of the background rate is not directly related to radon in the liquid¹⁰. Some of the low energy rate might be due to radon or radon daughters decaying in the neck of the detector, from where most of the scintillation light cannot reach the PMTs. These events would have pulse shapes that look like alpha events, however with much lower visible energy. In DEAP-3600, a plastic plug will be inserted in the neck to stop most of the UV light coming from the neck (this is also for shielding neutrons coming from the materials in the neck).

¹⁰ Note that this is not inconsistent with the SRIM calculations we showed in Table 2, where $\sim 11\%$ of ^{210}Po decays on the TPB inner surface leaks into WIMP energy region.

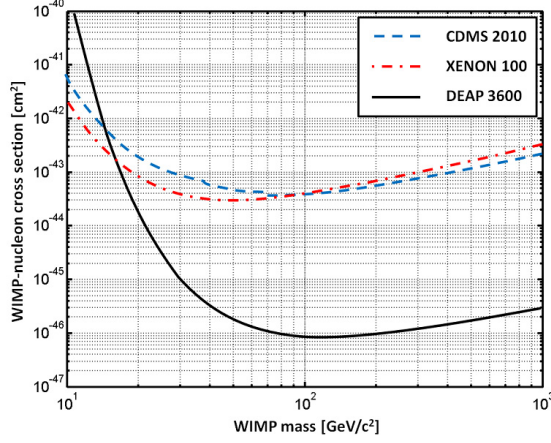


FIGURE 4. Experimental sensitivities for CDMS and XENON-100 (the current best limits), as well as the projected sensitivity for DEAP-3600

DEAP-3600 PHYSICS SENSITIVITY

The projected spin-independent WIMP-nucleon experimental sensitivity for DEAP-3600 is shown in Figure 4, compared to current results from CDMS [15] and XENON-100 [16]. It is assumed that we have a 20 keV_{ee} energy threshold and 3 years of livetime with 1000 kg of liquid argon in fiducial volume.

We can extrapolate surface backgrounds from DEAP-1 to DEAP-3600. The current background rate in the DEAP-1 detector is $\sim 130 \mu\text{Bq}$ with a 50% nuclear recoil acceptance. In the large detector, the background rate could scale with surface area if the backgrounds are from ^{210}Pb on the detector surfaces (noted as case 1). This gives

$$R_{3600} = \frac{130 \mu\text{Bq}}{50\%} \cdot \frac{9 \text{ m}^2}{0.2 \text{ m}^2} = 11.7 \text{ mBq} \quad (7)$$

where 9 m² and 0.2 m² are the detector inner surface areas for DEAP-3600 and DEAP-1, respectively. If we assume the backgrounds in the WIMP ROI are from radon emanation in the process systems (case 2), then we might expect the same level of backgrounds in DEAP-3600, since the process system will be similar. This means

$$R_{3600} = \frac{130 \mu\text{Bq}}{50\%} = 260 \mu\text{Bq} \quad (8)$$

Figure 5 shows the projected backgrounds in DEAP-3600 in the two cases as a function of fiducial volume, assuming 10-cm position resolution. With current DEAP-1 background rate, it would allow at least 230 kg background-free fiducial mass in DEAP-3600, which corresponds to a $4 \times 10^{-46} \text{ cm}^2$ WIMP-nucleon cross-section sensitivity around 100 GeV. Improvement in the background rate is expected due to the resurfacer, cleanliness control, etc., to achieve our target sensitivity.

SUMMARY

In this paper we discussed the background requirements for DEAP-3600 in order to reach its designed physics sensitivity. We have identified a list of surface background sources and for each source we have calculated the target level for various radioactive impurities. We need to ensure on the order of 10^{-12} g/g of material purity level in ^{238}U and ^{232}Th , which have been achieved by the SNO experiment, and 10^{-20} grams of ^{210}Pb per gram of material in the acrylic vessel or TPB wavelength shifter, which should be achievable with appropriate control of exposure to radon. We have plans to assay all relevant material radiopurity levels and will have Quality Assurance in place with AV manufacturer to assure a low radioimpurity level in the vessel. We are constructing a resurfacer device to remove surface contamination from the inner surface of the AV. We will develop a R&D program to purify TPB wavelength shifter and coating of it to the DEAP-3600 detector in the next year based on the existing knowledge and technique of acrylic purification and coating.

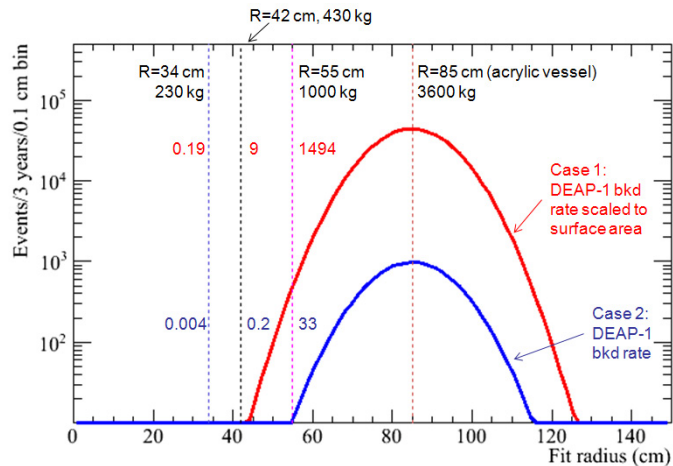


FIGURE 5. Projected backgrounds in DEAP-3600 with current DEAP-1 rates, assuming 10-cm position resolution. Case 1 is when surface backgrounds scale with detector surface, while case 2 assumes that backgrounds are from radon in the process system and we expect the same background rate in DEAP-3600 as DEAP-1

We have demonstrated significant background reduction with our prototype DEAP-1 detector and have good knowledge of where the remaining backgrounds are from. We have shown that even with the current background level in DEAP-1, we already have very competitive sensitivity in dark matter searches.

ACKNOWLEDGMENTS

This work is supported by the National Science and Engineering Research Council of Canada (NSERC), by the Canada Foundation for Innovation (CFI), by the Ontario Ministry of Research and Innovation (MRI), by the Queen's University, and by the David and Lucille Packard Foundation. We thank Wolfgang Rau for providing one of the figures.

REFERENCES

1. M. G. Boulay et al., arXiv:0904.2930 (2009)
2. D. Gastler et al., arXiv:1004.0373 (2010)
3. M. G. Boulay and A. Hime, *Astropart. Phys.* **25**, 179 (2006)
4. J. F. Ziegler, J. P. Biersack and U. Littmark, *The Stopping and Range of Ions in Solids*, Pergamon Press, New York (1985), new edition (2009)
5. T. Kat et al., *Nucl. Instrum. Methods. Phys. Res. A* **433**, 619 (1999)
6. T. Pollmann et al., arXiv:1011.1012 (2010)
7. J. L. Reyss et al., *Nucl. Instrum. Methods. Phys. Res. A* **357**, 391 (1995)
8. H. Nelder et al., *Applied Radiation and Isotop.* **53**, 191 (2000)
9. G. Heusser et al., *Proc. of Intern. Conf. Isotop. Environm. Studies Aquatic Forum*, Monte-Carlo, Monaco (2004)
10. D. Earle, R. Deal, and E. Gaudette, SNO-STR-93-042 (1994)
11. K. N. Yu and D. Nikezik, *Radiation Measurements* **41**, 101 (2006)
12. F. Duncan, *SNOLAB User's Handbook*, Revision 2 (2008)
13. M. Leung, *Proc. of Low Radioactivity Background Techniques*, Sudbury, ON, Canada (2004)
14. E. W. Hoppe et al., *Nucl. Instrum. Methods. Phys. Res. A* **579**, 486 (2007)
15. The CDMS II collaboration, *Science* **327**, 1619 (2010)
16. E. Aprile et al. (XENON100 collaboration), arXiv:1005.0380 (2010)